Inorganic Chemistry

pubs.acs.org/IC Article

Redox-Neutral Transformations of Carbon Dioxide Using Coordinatively Unsaturated Late Metal Silyl Amide Complexes

I. J. Huerfano, Carl A. Laskowski, Maren Pink, Veronica Carta, Gregory L. Hillhouse, Kenneth G. Caulton,* and Jeremy M. Smith*



Cite This: Inorg. Chem. 2022, 61, 20986-20993



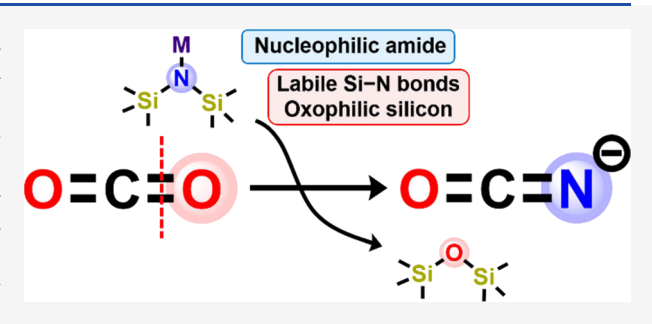
ACCESS I

III Metrics & More

Article Recommendations

s Supporting Information

ABSTRACT: Two-coordinate silylamido complexes of nickel and copper rapidly react with CO₂ to selectively form a new cyanate ligand along with hexamethyldisiloxane byproducts. Mechanistic insight into these reactions was obtained from the synthesis of proposed intermediates, several silyl- and phenyl- substituted amido analogues, and their subsequent reactivity with CO₂. These studies suggest that a unique intramolecular double silyl transfer step facilitates CO₂ deoxygenation, which likely contributes to the rapid rates of reaction. The deoxygenation reactions create a platform for a synthetic cycle in which copper amido complexes convert CO₂ to organic silylcarbamates.



INTRODUCTION

With growing atmospheric concentrations of carbon dioxide, the most well-known and abundant greenhouse gas, strategies for its conversion into useful chemical feedstocks have become an important yet unresolved challenge for chemists. Serving as the final thermodynamic carbon product for many important industrial and agricultural processes, such as the combustion of hydrocarbon fuels, modern energy, and consumer practices have had a direct negative impact on the planet's carbon economy. Without sufficient capacity for the consumption of anthropogenic carbon dioxide, natural systems are unable to compensate for their growing atmospheric presence.² This disruption of the natural carbon cycle has contributed toward significant ecological changes primarily in the form of climate change and ocean acidification which continue to persist as threats to the planet.^{3,4}

With its large environmental impact, high abundance, and challenging chemistry, CO_2 is a target of significant interest for metal-based catalysis as a C_1 building block for chemical fuels, specialty organic synthesis, and polymer materials. ^{5–10} The binding and activation of CO_2 by organometallic complexes have long been investigated. ¹¹ As the carbon core of CO_2 is in its highest oxidation state, most conversions targeted today are reductive transformations involving the addition of electrons and often some type of electrophile, typically protons. Three of the most common are reductive deoxygenation, hydrogenation, and reductive coupling. Often overlooked in comparison to reductive processes, redox-neutral transformations serve as an alternative route for the conversion of CO_2 into useful chemical feedstocks. These processes allow for reactivity that may circumvent some of the thermodynamic

challenges associated with reduction and can provide additional possibilities for synthetic applications of CO₂.

One important target is the conversion of CO₂ to organic isocyanates which are a more reactive form of carbon, able to rapidly react with alcohols and amines to form organic carbamates and urea. Exploiting this reactivity, diisocyanates can be used as monomer building blocks in reactions with diols or diamines to give polyurethanes and polyureas, respectively. These are both important materials used in many everyday products. For this reason, diisocyanates are industrially produced in millions of tons each year, primarily from phosgene, a toxic gas. Here, CO₂ may provide a safer and even cheaper alternative for the synthesis of isocyanates with the added benefit of environmental remediation.

The conversion of CO₂ to cyanate requires both a nucleophilic nitrogen source that attacks the electron-poor carbon core as well as an electrophile that facilitates the C–O bond cleavage and sequesters the oxygen atom. In this regard, the ambiphilicity of silylamido ligands makes them well poised for this transformation. Specifically, the anionic nitrogen provides the nucleophilic site, ^{15–18} while the labile Si–N bonds facilitate transfer of the electrophilic trimethylsilyl groups to oxygen. Furthermore, the inherent oxophilicity of silicon provides a strong thermodynamic driving force for

Received: September 29, 2022 Published: December 14, 2022





deoxygenation. For example, slow addition of CO_2 to the simple compound $\mathrm{NaN}(\mathrm{TMS})_2$ at slightly elevated temperatures results in the formation of small amounts of hexamethyldisiloxane (HMDSO) and NaNCO. However, these products are produced along with a mixture of other silylated carbon-containing compounds, highlighting a lack of selectivity. By contrast, silylamides of divalent group 14 elements (Ge and Sn) stoichiometrically form trimethylsilylisocyanate (TMSNCO) and siloxide-bridged Ge and Sn compounds at elevated pressures, highlighting the role of the metal in engendering selectivity.

There are now a handful of transition metal silyl amides that are known to react with CO_2 to form cyanates, where cyanate is either coordinated to the metal product or liberated as TMSNCO. However, in most cases, these reactions are slow with rates on the order of hours to days (Figure 1).^{23–29}

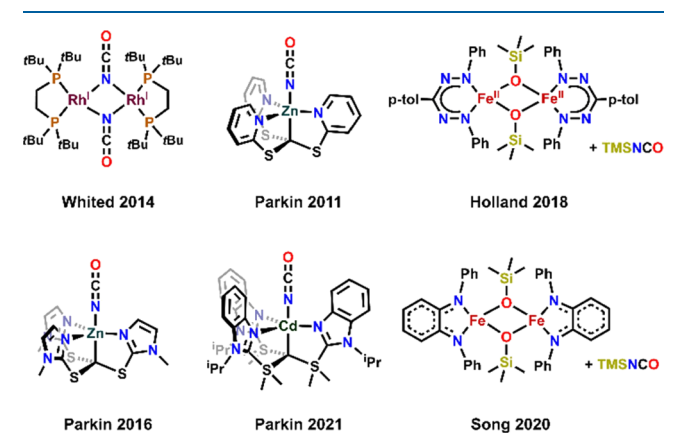


Figure 1. Previously reported cyanates derived from ${\rm CO_2}$ and transition metal trimethylsilylamides.

Notably, most of these reported examples contain electron-rich late transition metals. This property is particularly suited for channeling the desired reactivity because the higher d-electron count prevents π -donation from the lone pair on the amide ligand into an empty d-orbital, which would quench its nucleophilicity.

To this end, two-coordinate N-heterocyclic carbene (NHC) ligated silyl- and phenyl- substituted amide complexes of nickel and copper were synthesized for their reactivity toward CO₂. Lower coordination numbers are predicted to allow for more

facile reactivity with substrates due to the more accessible active site, and the unique monovalent nickel complex provides an especially intriguing framework for reactivity studies as its odd d-electron count makes it an unsaturated 13-electron species primed for reaction with substrates. Furthermore, lowvalent nickel systems have been demonstrated to be particularly good at CO₂ coordination, a possible initial mechanistic step before insertion. 11,30-33 Previous work in our group has already shown the capacity of monovalent nickel ligated with a silyl-containing PNP ligand to deoxygenate CO₂ at the expense of the ligand backbone,³⁴ making it an enticing choice for targeted reactivity with supporting ligand modifications. To evaluate the role of the highly reactive monovalent nickel center as well as other factors that may contribute to transformations of CO2 to cyanate, isostructural complexes of d10 monovalent copper were explored. In comparison to nickel, the monovalent oxidation state is typical for copper and tends to have lower reducing power due to its stable filled d-orbital configuration and lower overall orbital energy. Copper also provides the benefit of giving exclusively diamagnetic species in the absence of redox chemistry, allowing for facile characterization by NMR spectroscopy.

RESULTS AND DISCUSSION

Metal Silylamide Synthesis. As with the synthesis of IPrNiN(TMS)₂ (1),³⁵ analogous NHC-ligated copper silylamido complexes 2 and 3 are synthesized through salt metathesis reactions of LiN(TMS)2 with the corresponding (NHC)CuCl starting material (Scheme 1). The postulated two-coordinate linear geometry of 3 is confirmed by structural characterization using single crystal X-ray diffraction (Figure 2). With a C-Cu-N angle of $176.3(1)^{\circ}$, the two-coordinate linear geometry of 3 is very similar to that found in the analogous nickel complex 1 (178.71(9)°), confirming their isostructural character. The metal ligand bond distances in 3 are similar to those found in related monovalent copper complexes (see the SI).³⁶ The sum of the bond angles around the amido nitrogen atom reveals a nearly planar nitrogen (355°) likely due to steric effects as the amido lone pair is unable to donate into the filled π -symmetry d-orbitals of d¹⁰ Cu(I). Interestingly, the steric bulk of the trimethylsilyl groups is not fully impeded by the large mesityl substituents of the NHC, as evidenced by a dihedral angle of 55.5° between the two ligands, which is significantly less than the expected

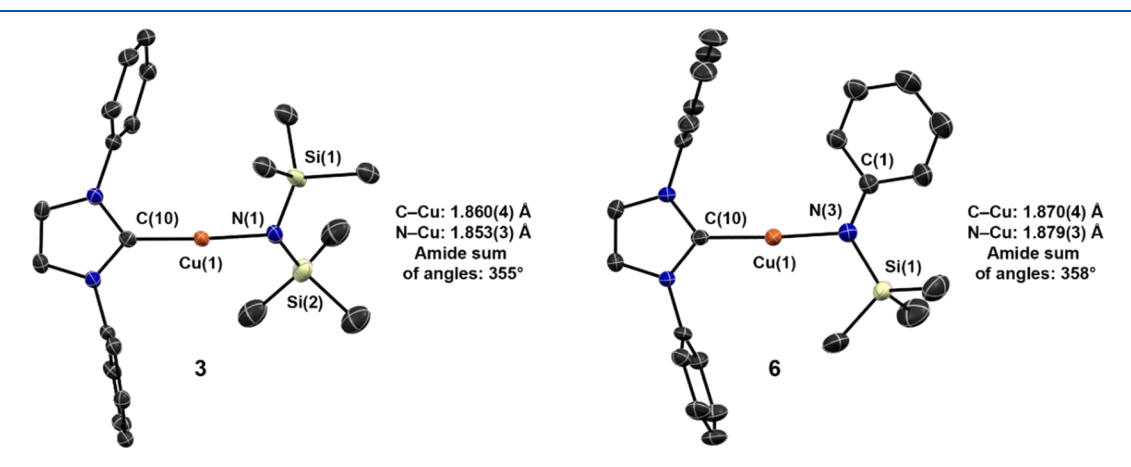


Figure 2. ORTEP representation of the molecular structure for 3 and 6. Thermal ellipsoids are shown at 30% probability. Hydrogen atoms and aryl substituents are omitted for clarity.

perpendicular arrangement. The ¹H- and ¹³C-NMR spectra are consistent with the solid-state structure, suggesting that the two-coordinate nature is maintained in solution. While 2 was not characterized by single crystal X-ray diffraction, ¹H- and ¹³C-NMR spectral characterizations for this complex are also consistent with the proposed linear geometry.

Scheme 1. Synthesis of 2-Coordinate Metal Amido Complexes (DIPP = 2,6-Diisopropylpheny, Mes = 2,4,6-Trimethylphenyl)

Ar = DIPP, R = TMS, R' = TMS (2) Ar = DIPP, R = Ph, R' = Ph (5) Ar = Mes, R = TMS, R' = TMS (3) Ar = DIPP, R = Ph, R' = TMS (6)

The previously reported diphenylamido nickel complex (4),³⁷ its copper analogue (5), as well as a copper trimethysilylphenylamido complex (6) were also synthesized from the appropriate metal halide and the corresponding lithium amido salt (Scheme 1) and fully characterized (see the SI). Structural characterization of 6 confirms the two-coordinate linear geometry with similar metal—ligand bonds and a similarly planar amido geometry (Figure 2).

Metal Cyanate Formation from CO₂. Addition of 1 equivalent of CO₂ to 1 in tetrahydrofuran (THF) at -78 °C results in a slight color change from yellow to light orange/yellow and the immediate formation of a new diamagnetic product, 7, together with stoichiometric hexamethyldisiloxane (HMDSO) (Scheme 2). The ¹H-NMR spectrum of the resulting nickel product indicates a highly symmetric species with only a single set of NHC signals between 1.0 and 8.5 ppm. The diamagnetism suggests the presence of a Ni–Ni bond, resulting from coupling of the single unpaired electron of each monovalent d⁹ metal, indicating a ligand-bridged dimeric species.

Crystals of 7 suitable for single-crystal X-ray diffraction were grown from a concentrated toluene solution layered with pentane and cooled to -40 °C. The solid-state structure reveals the original silylamidoligand to have successfully deoxygenated CO₂ to give an N-bound cyanate bridged dimer (Figure 3). The complex shows idealized two-fold symmetry in the solid-state with a close Ni–Ni distance consistent with previously reported monovalent nickel-bonded systems. Together, these data confirm the presence of a Ni–Ni bond consistent with diamagnetism observed in the NMR spectrum. The bond distances within the two NCO units are similar to those reported in other cyanate complexes and are therefore unperturbed by the bridging binding mode and the electron-rich monovalent nickel ions.

Unexpectedly, the solution IR spectrum of yellow/orange 7 in THF shows two strong vibrations at 2172 and 2203 cm⁻¹,

Scheme 2. Synthesis of Cyanate Complexes

DIPP

Nil-N

Nil-N

Si-

TMS₂O

DIPP

(1)

$$N_{i}^{i}$$

Nil-N

DIPP

(1)

 N_{i}^{i}
 N_{i}^{i}

Nil-N

DIPP

(7)

 N_{i}^{i}
 N_{i}^{i}

both characteristic of NCO (see the SI) and consistent with other metal cyanate complexes. 47-53 The IR spectrum of 7-N¹³CO, prepared using ¹³CO₂, gives the expected shift in frequency of these bands ($\nu_{\rm NCO}$ = 2113 and 2147 cm⁻¹, respectively), confirming CO2 as the carbon source of the cyanate ligand. The presence of two unique cyanate stretches in the IR spectrum suggests the presence of a possible dimermonomer or solvent adduct equilibrium in THF, as the idealized C_{2h} symmetric dimer should only give one signal based on IR selection rules. This hypothesis is supported by the spectrum of 7 obtained in benzene, which shows only a single cyanate stretch ($\nu_{\rm NCO}$ = 2172 cm⁻¹). This hypothesis is further supported by significant broadening of signals and loss of observable coupling in the ¹H- and ¹³C-NMR spectra when recorded in THF-d₈ rather than C₆D₆. Peak broadening further results in the absence of an observable cyanate signal by ¹³C-NMR spectroscopy in THF-d₈ and the region associated with metal cyanates is obscured by the residual carbon signals of C_6D_{61} making direct observation of the N¹³CO in 7-N¹³CO by NMR impossible.

Further confirmation for the identity of 7 comes from an independent synthesis of the cyanate complex (Scheme 2). The reaction of (IPrNiCl)₂ with KOCN affords a yellow powder whose 1 H- and 13 C-NMR spectra, as well as IR spectra are identical to the product obtained from the reaction of 1 with CO₂.

Likewise, the copper complexes 2 and 3 react with 1 atm of CO₂ at room temperature to afford the analogous cyanate complexes 8 and 9, respectively. Stoichiometric formation of HMDSO is observed in both reactions (Scheme 2). Single crystals of 8 and 9 suitable for X-ray diffraction were both grown from concentrated THF solutions layered with pentane and cooled to -40 °C, revealing (Figure 3) the formation of monomeric copper cyanate complexes. The bond lengths within the NCO ligand are similar to those found in the dimeric nickel analogue and typical of other reported metal

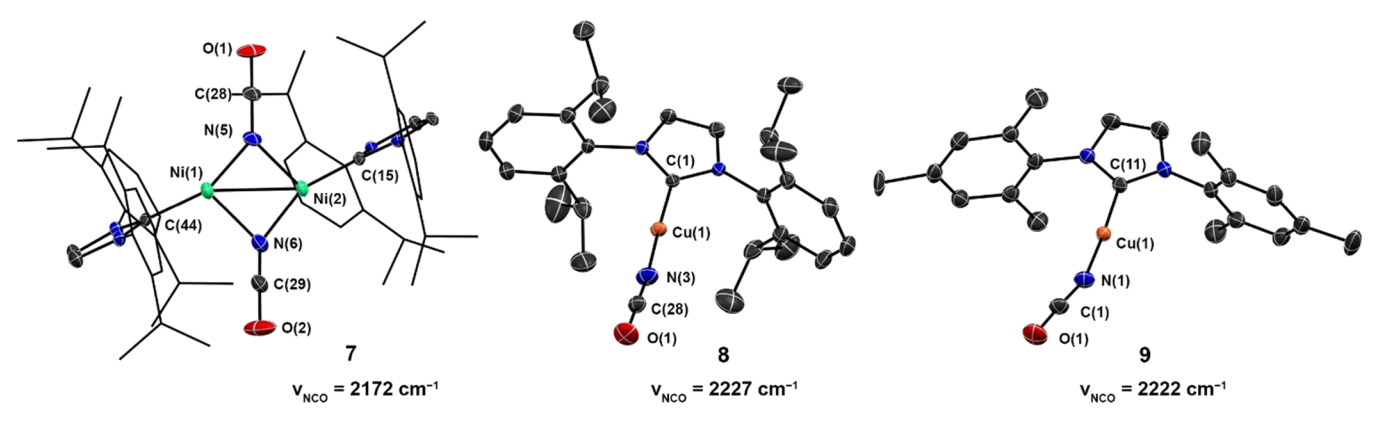


Figure 3. ORTEP representations of the molecular structures for 7-9. Thermal ellipsoids are shown at 30% probability. Diiso-propylphenyl groups in 7 are displayed as wireframes and hydrogen atoms are all omitted for clarity.

cyanates. ⁵⁴ Interestingly, while the Cu–N–C linkage is linear in 8 (175.1(3)°), in complex 9, it shows significant bending (160.0(6)°). Linear coordination of triatomic ligands such as cyanate is generally attributed to π -donation of a ligand lone pair to empty metal d-orbitals or back-bonding from the metal to an empty ligand π^* orbital. Neither is likely in these complexes: the filled d¹⁰ electron configuration of monovalent copper prevents π -donation from the ligand, and the low energy of its filled orbitals makes copper(I) poor at back-bonding. Together, this suggests that the difference in bond angles is steric in nature and likely a result of molecular packing in the crystal.

The solution ¹H-NMR spectra for 8 and 9 are consistent with complexes having twofold symmetry, supporting the hypothesis that Cu–N–C bending is a solid-state effect. The solution IR spectra each show a single NCO stretch, which, together with the NMR data, suggests that 8 and 9 maintain their two-coordinate monomeric geometry in solution in contrast to the nickel analogue. Synthesis of 8-N¹³CO using 13 CO₂ results in the expected shift in the cyanate stretch from 2227 to 2167 cm⁻¹, confirming CO₂ as the source of carbon. The 13 C-NMR spectrum of 8-N¹³CO in THF-d₈ shows a new broad signal at 125 ppm, consistent with a CO₂-derived cyanate. ⁵⁵ The broadness of the peak is attributed to coupling with the adjacent 14 N nucleus ($I_N = 1$).

The work presented demonstrates the first example of selective cyanate formation from CO₂ using a molecular Cu(I) species. This is notable because other Cu(I) complexes have been observed to favor reductive coupling to oxalate. 56,57 This result also demonstrates that strongly reducing metal complexes, such as those based on Ni(I), are not required for conversion to cyanate and suggests that the nucleophilicity of the amido ligand is more important for CO2 capture and conversion. It is worth noting, however, that the rates of reaction for 1 are qualitatively faster than those observed for 2 and 3, This observation possibly could be due to coordination of CO₂ to nickel, allowing a lower barrier pathway than that attainable by copper or simply that the nickel amido is more nucleophilic than its copper analogue. Nonetheless, the twocoordinate copper complexes react significantly faster than the previously reported complexes, suggesting the importance of low coordination numbers for cyanate formation.

Mechanistic Investigation into Cyanate Formation. Based on the consensus mechanism for CO₂ deoxygenation and nitrogen transfer involving metal trimethylsilylamido complexes (Scheme 3; pathway A), ^{28,29} we targeted the

Scheme 3. Proposed Mechanistic Pathways for Cyanate Formation

$$L-M-N \xrightarrow{Si-} CO_2 \qquad L-M \xrightarrow{O} C-N \xrightarrow{Si-} L-M \xrightarrow{O} CO_2 \qquad L-M \xrightarrow{O} CO_2 \qquad L-M \xrightarrow{O} CO_2 \qquad L-M-O \xrightarrow{Si-} III$$

synthesis and reactivity of likely intermediates for the reactions of complexes 1–3. In contrast to previous examples, the fast rates of these two-coordinate nickel and copper complexes have precluded the direct isolation and characterization of any reaction intermediates.

The transformation to cyanate is proposed to begin with initial CO₂ insertion into the metal-nitrogen bond (I), which is then followed by rapid silyl group migration to an oxygen atom in the newly formed carboxylate ligand, as driven by the inherent oxophilicity of silicon (II). This provides an Osilylcarbamate ligand, which has previously been found to rapidly eject TMSNCO, affording a metal siloxide complex (III). In the case of the reported Fe-formazanate²⁴ and Fephenylenediamide²³ complexes shown in Figure 1, this is the terminal step of the reaction, providing isolable bridging siloxide complexes along with TMSNCO. In contrast, rhodium,²⁹ zinc,^{27,28} and cadmium^{25,26} examples (Figure 1) form metal siloxides which react further with the released TMSNCO to generate the final metal-cyanate complex. Although final metal cyanate formation only appears to require a simple σ -bond metathesis reaction with the free TMSNCO, this reaction has not been previously observed to occur at a rate compatible with the overall transformation, despite the expected thermodynamic favorability. Metathesis is generally only observed in the presence of excess CO₂ enabled by an

additional insertion of the siloxide intermediate to form a silyl-carbonate complex (IV). It is speculated that the large trimethylsiloxide ligand is too sterically bulky and blocks the metal from metathesis reactions.

We probed the initial association of CO_2 to complexes 1-3(I) using the diphenylamido analogues 4 and 5, where the absence of silyl groups is expected to inhibit downstream deoxygenation steps. Stoichiometric addition of CO₂ to 4 at -78 °C in Et₂O initiates a dramatic color change from dark blue to red which reverts back to blue upon warming of the reaction mixture, implying a reversible CO2 association process. Monitoring this process by VT-IR spectroscopy shows the appearance of two new features at 2229 and 2295 cm⁻¹ below 253 K (see the SI), both of which disappear when warmed to 263 K. These frequencies are at slightly lower energy than that of the antisymmetric C=O vibration of free CO₂ (~2340 cm⁻¹). Similarly, VT-NMR of 5 under 1 atm of CO₂ suggests the reversible association of CO₂. Here, lowering the temperature results in the appearance of resonances for a twofold symmetric complex. The concentration of this new species, tentatively assigned as $IPrCu(CO_2)(NPh_2)$ (5·CO₂), increases with decreasing temperature (see the SI). Importantly, warming results in the loss of these signals, with complete conversion back to 5.

With evidence for the weak binding of CO₂ to the amido complexes, we investigated the subsequent silyl migration (II) and deoxygentation (III) steps. Analysis of the proposed mechanism led us to hypothesize that a phenylsilylamido ligand would divert the reaction to yield phenylisocyanate along with 10. Surprisingly, the reaction of 6 with CO2 does not result in the stoichiometric formation of phenylisocyanate and 10 but instead undergoes complete conversion to a new metal-containing product, 11, which can be isolated as a white solid. The ¹H- and ¹³C-NMR spectra are consistent with a new diamagnetic complex containing an intact NHC ligand as well as both phenyl and trimethylsilyl groups distinct from the amido starting material in appropriate integration. Notably, the protons assigned to the phenyl substituent of the initial amido ligand shift downfield now ranging from 6.8 to 7.4 ppm compared to 6.0–6.7 ppm in the starting material (see the SI), consistent with the greater electron-withdrawing capabilities of a CO₂-derived carbamate compared to the initial amido ligand. The natural abundance ¹³C-NMR spectrum of 11 shows a resonance at 160 ppm, consistent with the region associated with organic carbamates⁵⁸ with peak intensity increasing dramatically when the complex is prepared from ¹³CO₂. These observations suggest the formation of a carbamate from CO₂ and indicates that CO₂ inserts into the amido ligand of 6 (Scheme 4). The proposed structure for 11 is based on the demonstrated propensity for NHC-ligated copper complexes to adopt a two-coordinate linear geometry, the symmetry observed in the NMR spectra, and IR spectroscopy showing a new stretch at 1632 cm⁻¹ characteristic of a C=O bond in the newly formed carbamate ligand.

Attempts to thermally induce the release of phenylisocyanate from 11 were unsuccessful. To determine whether this lack of reactivity was thermodynamic or kinetic in nature, we further investigated the siloxide complex IPrCuOTMS, which is the anticipated copper product of phenylisocyanate liberation from 11. The two-coordinate complex (10) is readily synthesized from IPrCuCl and NaOTMS (Scheme 5) and fully characterized by single crystal X-ray diffraction and solution spectroscopic methods (see the SI for more details).

Scheme 4. Synthesis of Copper-Carbamate and Reactivity with TMSCl

Scheme 5. Synthesis and Reactivity of a Copper Siloxide Complex

Treating 10 with phenylisocyanate results in the quantitative formation of 11, indicating that phenylisocyanate liberation is thermodynamically unfavorable. Considering this observation, we also investigated the reaction of 10 with TMSNCO (Scheme 5). In this case, complete conversion to the cyanate complex 8 and HMDSO occurs within ten minutes, as evaluated by $^1\text{H-NMR}$ spectroscopy. In addition, we do not observe any reaction between 10 and CO_2 . These observations lead to the conclusion that a second insertion step (IV) does not occur in the mechanism for cyanate formation in the NHC-supported two-coordinate systems and is inconsistent with mechanism A.

We therefore propose that double silyl transfer is required for the complete deoxygenation of CO2 to cyanate and likely proceeds through this second silyl transfer step before undergoing direct loss of HMDSO rather than releasing TMSNCO and reincorporating the cyanate ligand through subsequent metathesis reactions (Scheme 3, pathway B). After the initial insertion of CO₂, this proposed mechanism may also account for faster reaction rates observed for complexes 1-3. In previous examples, the rate-limiting steps are proposed to be either the insertion of a second molecule of CO₂ prior to σ bond metathesis, likely due to the decreased nucleophilicity of the siloxide ligand in comparison to the amido or the final σ bond metathesis itself. In the case of the two-coordinate complexes reported here, deoxygenation by the proposed double silyl transfer pathway is intramolecular, accounting for the faster reaction rates.

Synthetic Cycle for CO₂ Functionalization. With deoxygenation necessitating double silyl transfer, we speculated that 11 may itself serve as a precursor to phenylisocyanate through the addition of a second silyl source. This hypothesis was tested by treating 11 with ¹³CO₂ and excess TMSCl in C₆D₆. Interestingly, the ¹H-NMR spectrum of this reaction does not show the formation of phenyl isocyanate but is instead consistent with the known bis(silyl)phenylcarbamate $Ph(Me_3Si)NC(O)OSiMe_3$ (see the SI). The $^{13}C-NMR$ spectrum of this product confirms that the added CO2 gas is incorporated in the final organic product, with high-intensity resonance at 160 ppm. The reaction also results in the precipitation of a white solid, which is confirmed to be IPrCuCl by NMR spectroscopy. This reaction therefore closes a synthetic cycle for the conversion of LiN(Ph)(TMS), CO₂, and TMSCl to the previously reported bis(silyl)phenylcarbamate (12) (Scheme 6). Bis(silyl)carbamates such as 12 have recently been demonstrated to transform to isocyanate and HMDSO under thermal conditions;⁵⁹ thus, this synthetic cycle may provide a new avenue toward CO2-derived organic isocyanates.

Scheme 6. Complete Synthetic Cycle for the Conversion of LiNPhTMS with ${\rm CO_2}$

CONCLUSIONS

In this work, the reactivity of CO_2 with two-coordinate complexes of nickel and copper-containing silyl- and phenyl-substituted amido ligands was investigated. Reactions of the bis(silyl)amido complexes 1-3 resulted in clean and fast conversion to the corresponding metal cyanate complexes, which are formed in high yields. Analogous reactivity of the related phenyl-substituted amides 4 and 5 provided important mechanistic insight into this deoxygenation process. In addition, the reactivity of a siloxide complex, 10, was evaluated for its competency as a reaction intermediate in CO_2 conversion.

Together, these investigations suggest that a multistep mechanism for the reaction of CO_2 with a metal silylamido similar to those proposed for other complexes is unlikely to be operative. Instead, we hypothesize an alternative mechanism involving double N-to-O silyl transfer that facilitates the rapid deoxygenation of a carbamate intermediate to afford the final cyanate complex. Finally, a complete synthetic cycle for the synthesis of an organic bis(silyl)carbamate, 12, was established through the reaction of CO_2 with 6 in the presence of TMSCl as an additional silyl source. As silyl carbamates can be thermally transformed into organic isocyanates, this result provides early optimism for the prospect of utilizing CO_2 as a feedstock for building blocks used to make many common polymers.

ASSOCIATED CONTENT

Supporting Information

The Supporting Information is available free of charge at https://pubs.acs.org/doi/10.1021/acs.inorgchem.2c03453.

Synthesis and characterization, including copies of spectra (PDF)

Accession Codes

CCDC 2210074–2210076 and 2210084–2210086 contain the supplementary crystallographic data for this paper. These data can be obtained free of charge via www.ccdc.cam.ac.uk/data_request/cif, or by emailing data_request@ccdc.cam.ac.uk, or by contacting The Cambridge Crystallographic Data Centre, 12 Union Road, Cambridge CB2 1EZ, UK; fax: +44 1223 336033.

AUTHOR INFORMATION

Corresponding Authors

Kenneth G. Caulton — Department of Chemistry, Indiana University, Bloomington, Indiana 47405, United States; orcid.org/0000-0003-3599-1038; Email: caulton@indiana.edu

Jeremy M. Smith — Department of Chemistry, Indiana University, Bloomington, Indiana 47405, United States; orcid.org/0000-0002-3206-4725; Email: smith962@indiana.edu

Authors

I. J. Huerfano — Department of Chemistry, Indiana University, Bloomington, Indiana 4740S, United States

Carl A. Laskowski – Department of Chemistry, University of Chicago, Chicago, Illinois 60637, United States

Maren Pink – Department of Chemistry, Indiana University, Bloomington, Indiana 47405, United States; orcid.org/0000-0001-9049-4574

Veronica Carta — Department of Chemistry, Indiana University, Bloomington, Indiana 47405, United States *Gregory L. Hillhouse — Department of Chemistry, University of Chicago, Chicago, Illinois 60637, United States

Complete contact information is available at: https://pubs.acs.org/10.1021/acs.inorgchem.2c03453

Notes

The authors declare no competing financial interest. §Deceased March 6, 2014.

ACKNOWLEDGMENTS

This research was supported by the National Science Foundation, Chemical Synthesis Program (SYN), by grant CHE-1362127 to K.G.C. Support for the acquisition of the Bruker Venture D8 diffractometer through the Major Scientific Research Equipment Fund from the President of Indiana University and the Office of the Vice President for Research is gratefully acknowledged. NSF's ChemMatCARS Sector 15 is principally supported by the Divisions of Chemistry (CHE) and Materials Research (DMR). We thank Prof. Vlad Illuc (Notre Dame) for connecting the research groups.

REFERENCES

- (1) Climate Change Indicators: Atmospheric Concentration of Greenhouse Gases. https://www.epa.gov/climate-indicators/climate-change-indicators-atmospheric-concentrations-greenhouse-gases#ref5.
- (2) Canadell, J. G.; Le Quéré, C.; Raupach, M. R.; Field, C. B.; Buitenhuis, E. T.; Ciais, P.; Conway, T. J.; Gillett, N. P.; Houghton, R. A.; Marland, G. Contributions to accelerating atmospheric CO₂ growth from economic activity, carbon intensity, and efficiency of natural sinks. *Proc. Natl. Acad. Sci. U. S. A.* **2007**, *104*, 18866–18870.
- (3) Friedlingstein, P.; Andrew, R. M.; Rogelj, J.; Peters, G. P.; Canadell, J. G.; Knutti, R.; Luderer, G.; Raupach, M. R.; Schaeffer, M.; van Vuuren, D. P.; Le Quere, C. Persistent growth of CO₂ emissions and implications for reaching climate targets. *Nat. Geosci.* **2014**, *7*, 709–715
- (4) Gattuso, J.-P.; Magnan, A.; Billé, R.; Cheung, W. W. L.; Howes, E. L.; Joos, F.; Allemand, D.; Bopp, L.; Cooley, S. R.; Eakin, C. M.; Hoegh-Guldberg, O.; Kelly, R. P.; Pörtner, H.-O.; Rogers, A. D.; Baxter, J. M.; Laffoley, D.; Osborn, D.; Rankovic, A.; Rochette, J.; Sumaila, U. R.; Treyer, S.; Turley, C. OCEANOGRAPHY. Contrasting futures for ocean and society from different anthropogenic CO₂ emissions scenarios. *Science* 2015, 349, No. aac4722.
- (5) Kinzel, N. W.; Werlé, C.; Leitner, W. Transition Metal Complexes as Catalysts for the Electroconversion of CO₂: An Organometallic Perspective. *Angew. Chem., Int. Ed.* **2021**, *60*, 11628–11686.
- (6) Yin, X.; Moss, J. R. Recent developments in the activation of carbon dioxide by metal complexes. *Coord. Chem. Rev.* **1999**, *181*, 27–59.
- (7) Taylor, L. J.; Kays, D. L. Low-coordinate first-row transition metal complexes in catalysis and small molecule activation. *Dalton Trans.* **2019**, *48*, 12365–12381.
- (8) Kubiak, C. P.; Ratliff, K. S. Approaches to the Chemical, Electrochemical, and Photochemical Activation of Carbon Dioxide by Transition Metal Complexes. *Isr. J. Chem.* **1991**, *31*, 3–15.
- (9) Mason, M. G.; Ibers, J. A. Reactivity of some transition metal systems toward liquid carbon dioxide. *J. Am. Chem. Soc.* **1982**, *104*, 5153–5157.
- (10) Liu, Q.; Wu, L.; Jackstell, R.; Beller, M. Using carbon dioxide as a building block in organic synthesis. *Nat. Commun.* **2015**, *6*, 5933.
- (11) Aresta, M. Carbon Dioxide Reduction and Uses as a Chemical Feedstock. In *Activation of Small Molecules*; Wiley: 2006; pp. 1–41.
- (12) Six, C.; Richter, F. Isocyanates, Organic. In Ullmann's Encyclopedia of Industrial Chemistry; Wiley: 2003.
- (13) Richter, R.; Ulrich, H. Syntheses and preparative applications of isocyanates. In *Cyanates and Their Thio Derivatives* (1977); Wiley: 1977; pp. 619–818.
- (14) Sonnenschein, M. F. Introduction. In *Polyurethanes*; Wiley: 2014; pp. 1–9.
- (15) Andersen, R. A. Dialkylbis[bis(trimethylsilyl)amido] zirconium(IV) and -hafnium(IV). Preparation and reaction with carbon dioxide and tert-butylisocyanide. *Inorg. Chem.* **1979**, *18*, 2928–2932.
- (16) Chisholm, M. H.; Cotton, F. A.; Extine, M. W.; Rideout, D. C. Reactions of transition-metal-nitrogen σ -bonds. 5. Carbonation of tetrakis(diethylamido)chromium(IV) to yield binuclear chromium-

- (III) and -(II) carbamato complexes. Inorg. Chem. 1978, 17, 3536-3540.
- (17) Chisholm, M. H.; Extine, M. Reactions of transition metalnitrogen σ -bonds. II. Pentakis(N,N-dimethylcarbamato) niobium(V) and its facile exchange reaction with carbon dioxide. *J. Am. Chem. Soc.* 1975, 97, 1623–1625.
- (18) Tang, Y.; Zakharov, L. N.; Rheingold, A. L.; Kemp, R. A. Insertion of Carbon Dioxide into Mg–N Bonds. Structural Characterization of a Previously Unknown η^2 Chelation Mode to Magnesium in Magnesium Carbamates. *Organometallics* **2004**, 23, 4788–4791.
- (19) Wannagat, U.; Kuckertz, H.; Krüger, C.; Pump, J. Beiträge zur Chemie der Silicium-Stickstoff-Verbindungen. XXXVIII. Reaktionen des Natrium-bis-[trimethylsilyl]-amids mit Kohlenstoffchalkogeniden und Kohlenstoffhalogeniden. Z. Anorg. Allg. Chem. 1964, 333, 54–61.
- (20) Rimo, X.; Sita, L. R. Mechanistic details for metathetical exchange between XCO (X = O and RN) and the tin(II) dimer, $\{Sn[N(SiMe_3)_2] (\mu-OBut)\}_2$. Inorg. Chim. Acta 1998, 270, 118–122.
- (21) Sita, L. R.; Babcock, J. R.; $\dot{X}i$, R. Facile Metathetical Exchange between Carbon Dioxide and the Divalent Group 14 Bisamides $M[N(SiMe_3)_2]_2$ (M = Ge and Sn). *J. Am. Chem. Soc.* **1996**, *118*, 10912–10913.
- (22) Babcock, J. R.; Sita, L. R. Facile Preparation of Unsymmetric Carbodiimides via in Situ Tin(II)-Mediated Heterocumulene Metathesis. *J. Am. Chem. Soc.* **1998**, *120*, 5585–5586.
- (23) Broere, D. L. J.; Mercado, B. Q.; Holland, P. L. Selective Conversion of CO₂ into Isocyanate by Low-Coordinate Iron Complexes. *Angew. Chem., Int. Ed.* **2018**, *57*, 6507–6511.
- (24) Liang, Q.; Lin, J. H.; DeMuth, J. C.; Neidig, M. L.; Song, D. Syntheses and characterizations of iron complexes of bulky ophenylenediamide ligand. *Dalton Trans.* **2020**, 49, 12287–12297.
- (25) Chakrabarti, N.; Ruccolo, S.; Parkin, G. Cadmium Compounds with an [N₃C] Atrane Motif: Evidence for the Generation of a Cadmium Hydride Species. *Inorg. Chem.* **2016**, *55*, 12105–12109.
- (26) Hammond, M.; Rauch, M.; Parkin, G. Synthesis, Structure, and Reactivity of a Terminal Cadmium Hydride Compound, [κ_3 -TismPriBenz]CdH. *J. Am. Chem. Soc.* **2021**, *143*, 10553–10559.
- (27) Ruccolo, S.; Sattler, W.; Rong, Y.; Parkin, G. Modulation of Zn–C Bond Lengths Induced by Ligand Architecture in Zinc Carbatrane Compounds. J. Am. Chem. Soc. 2016, 138, 14542–14545.
- (28) Sattler, W.; Parkin, G. Synthesis, Structure, and Reactivity of a Mononuclear Organozinc Hydride Complex: Facile Insertion of CO₂ into a Zn–H Bond and CO₂-Promoted Displacement of Siloxide Ligands. *J. Am. Chem. Soc.* **2011**, *133*, 9708–9711.
- (29) Whited, M. T.; Kosanovich, A. J.; Janzen, D. E. Synthesis and Reactivity of Three-Coordinate (dtbpe)Rh Silylamides: CO₂ Bond Cleavage by a Rhodium(I) Disilylamide. *Organometallics* **2014**, 33, 1416–1422.
- (30) Chiou, T.-W.; Tseng, Y.-M.; Lu, T.-T.; Weng, T.-C.; Sokaras, D.; Ho, W.-C.; Kuo, T.-S.; Jang, L.-Y.; Lee, J.-F.; Liaw, W.-F. [Ni^{III}(OMe)]-mediated reductive activation of CO_2 affording a Ni(κ^1 -OCO) complex. *Chem. Sci.* **2016**, *7*, 3640–3644.
- (31) Aresta, M.; Nobile, C. F.; Albano, V. G.; Forni, E.; Manassero, M. New nickel—carbon dioxide complex: synthesis, properties, and crystallographic characterization of (carbon dioxide)-bis-(tricyclohexylphosphine)nickel. *J. Chem. Soc., Chem. Commun.* 1975, 636–637.
- (32) Aresta, M.; Nobile, C. F. (Carbon dioxide) bis-(trialkylphosphine)nickel complexes. *J. Chem. Soc., Dalton Trans.* 1977, 708–711.
- (33) Doehring, A.; Jolly, P. W.; Krueger, C.; Romao, M. J. The nickel(0)-carbon dioxide system: structure and reactions of [Ni-(PCy₃)₂(η^2 -CO₂)]. Z. Naturforsch. B: Anorg. Chem. Org. Chem. 1985, 40B, 484–488.
- (34) Fullmer, B. C.; Fan, H.; Pink, M.; Caulton, K. G. O/C Bond Cleavage of CO₂ by Ni¹. *Inorg. Chem.* **2008**, 47, 1865–1867.
- (35) Laskowski, C. A.; Hillhouse, G. L. Two-Coordinate d⁹ Complexes. Synthesis and Oxidation of NHC Nickel(I) Amides. *J. Am. Chem. Soc.* **2008**, *130*, 13846–13847.

- (36) Coyle, J. P.; Sirianni, E. R.; Korobkov, I.; Yap, G. P. A.; Dey, G.; Barry, S. T. Study of Monomeric Copper Complexes Supported by N-Heterocyclic and Acyclic Diamino Carbenes. *Organometallics* **2017**, 36, 2800–2810.
- (37) Inatomi, T.; Fukahori, Y.; Yamada, Y.; Ishikawa, R.; Kanegawa, S.; Koga, Y.; Matsubara, K. Ni(I)—Ni(III) cycle in Buchwald—Hartwig amination of aryl bromide mediated by NHC-ligated Ni(I) complexes. *Catal. Sci. Technol.* **2019**, *9*, 1784—1793.
- (38) Dürr, A. B.; Fisher, H. C.; Kalvet, I.; Truong, K.-N.; Schoenebeck, F. Divergent Reactivity of a Dinuclear (NHC)Nickel(I) Catalyst versus Nickel(0) Enables Chemoselective Trifluoromethylselenolation. *Angew. Chem., Int. Ed.* **2017**, *56*, 13431–13435.
- (39) Zhou, Y.-Y.; Uyeda, C. Reductive Cyclopropanations Catalyzed by Dinuclear Nickel Complexes. *Angew. Chem., Int. Ed.* **2016**, *55*, 3171–3175.
- (40) Koch, F.; Berkefeld, A.; Schubert, H.; Grauer, C. Redox and Acid-Base Properties of Binuclear 4-Terphenyldithiophenolate Complexes of Nickel. *Chem. Eur. J.* **2016**, 22, 14640–14647.
- (41) Dible, B. R.; Sigman, M. S.; Arif, A. M. Oxygen-Induced Ligand Dehydrogenation of a Planar Bis- μ -Chloronickel(I) Dimer Featuring an NHC Ligand. *Inorg. Chem.* **2005**, *44*, 3774–3776.
- (42) Wang, Q.; Zhang, S.; Cui, P.; Weberg, A. B.; Thierer, L. M.; Manor, B. C.; Gau, M. R.; Carroll, P. J.; Tomson, N. C. Interdependent Metal—Metal Bonding and Ligand Redox-Activity in a Series of Dinuclear Macrocyclic Complexes of Iron, Cobalt, and Nickel. *Inorg. Chem.* 2020, 59, 4200–4214.
- (43) Peng, S.-M.; Goedken, V. L. Cofacial dimer of a dihydrooctaaza[14]annulene complex containing a nickel-nickel bond and related monomeric complexes. *J. Am. Chem. Soc.* **1976**, 98, 8500–8510.
- (44) Bach, I.; Goddard, R.; Kopiske, C.; Seevogel, K.; Pörschke, K.-R. Synthesis, Structure, and Reactivity of $(tBu_2PC_2H_4PtBu_2)Ni(CH_3)_2$ and $\{(tBu_2PC_2H_4PtBu_2)Ni\}_2(\mu-H)_2$. Organometallics 1999, 18, 10–20.
- (45) Jones, R. A.; Norman, N. C.; Seeberger, M. H.; Atwood, J. L.; Hunter, W. E. Synthesis and x-ray crystal structure of $[M(\mu-(Me_3C)(H)P)(PMe_3)_2]_2$ (M = Rh, Ni) containing rhodium:rhodium double and nickel-nickel single bonds. *Organometallics* **1983**, 2, 1629–1634.
- (46) Jones, R. A.; Stuart, A. L.; Atwood, J. L.; Hunter, W. E. Substitution reactions of di-tert-butylphosphido complexes of nickel-(I). Crystal structures of $Ni_2[\mu-(Me_3C)_2P]_2(CO)_2(PMe_3)$ (Ni-Ni) and $Ni_2[\mu-(Me_3C)_2P]_2(CO)_3$ (Ni-Ni). Organometallics 1983, 2, 874–878.
- (47) Bröring, M.; Prikhodovski, S.; Brandt, C. D.; Cónsul Tejero, E. Pillars, Layers, Pores and Networks from Nickeltripyrrins: A Porphyrin Fragment as a Versatile Building Block for the Construction of Supramolecular Assemblies. *Chem. Eur. J.* **2007**, 13, 396–406.
- (48) Dey, S. K.; Mondal, N.; El Fallah, M. S.; Vicente, R.; Escuer, A.; Solans, X.; Font-Bardía, M.; Matsushita, T.; Gramlich, V.; Mitra, S. Crystal Structure and Magnetic Interactions in Nickel(II) Dibridged Complexes Formed by Two Azide Groups or by Both Phenolate Oxygen—Azide, —Thiocyanate, —Carboxylate, or —Cyanate Groups. *Inorg. Chem.* 2004, 43, 2427—2434.
- (49) Habib, M.; Karmakar, T. K.; Aromí, G.; Ribas-Ariño, J.; Fun, H.-K.; Chantrapromma, S.; Chandra, S. K. A Versatile Series of Nickel(II) Complexes Derived from Tetradentate Imine/Pyridyl Ligands and Various Pseudohalides: Azide and Cyanate Compared. *Inorg. Chem.* 2008, 47, 4109–4117.
- (50) Vicente, R.; Escuer, A.; El Fallah, M. S.; Solans, X.; Font-Bardia, M. Three new mononuclear nickel(II) cyanate and isocyanate compounds derived from macrocyclic ligands: [Ni(TMCY) (NCO)]-(ClO₄), [Ni(m-CTH)(OCN)_{1.5}(ClO₄)_{0.5}]. *Inorg. Chim. Acta* **1997**, 261, 227–232.
- (51) Lefèvre, X.; Spasyuk, D. M.; Zargarian, D. New POCOP-type pincer complexes of Nickel(II). *J. Organomet. Chem.* **2011**, *696*, 864–870.

- (52) Panja, A.; Jana, N. C.; Adak, S.; Brandão, P.; Dlháň, L.; Titiš, J.; Boča, R. The structure and magnetism of mono- and di-nuclear Ni(II) complexes derived from {N₃O}-donor Schiff base ligands. *New J. Chem.* **2017**, *41*, 3143–3153.
- (53) Jana, S.; Bhaumik, P. K.; Harms, K.; Chattopadhyay, S. Synthesis, characterization and DFT study of nickel(II) complexes of a N₂O donor Schiff base with different pseudo-halides: Formation of supra-molecular architectures by $C-H\cdots\pi$ interactions. *Polyhedron* **2014**, 78, 94–103.
- (54) Dodds, C. A.; Kennedy, A. R.; Thompson, R. Taming Copper(I) Cyanate and Selenocyanate with N-Heterocyclic Carbenes. *Eur. J. Inorg. Chem.* **2019**, 2019, 3581–3587.
- (55) Bialas, N.; Höcker, H.; Marschner, M.; Ritter, W. ¹³C NMR studies on the relative reactivity of isocyanate groups of isophorone diisocyanate isomers. *Makromol. Chem.* **1990**, *191*, 1843–1852.
- (56) Cook, B. J.; Di Francesco, G. N.; Abboud, K. A.; Murray, L. J. Countercations and Solvent Influence CO₂ Reduction to Oxalate by Chalcogen-Bridged Tricopper Cyclophanates. *J. Am. Chem. Soc.* **2018**, 140, 5696–5700.
- (57) Angamuthu, R.; Byers, P.; Lutz, M.; Spek, A. L.; Bouwman, E. Electrocatalytic CO₂ Conversion to Oxalate by a Copper Complex. *Science* **2010**, 327, 313–315.
- (58) Olah, G. A.; Heiner, T.; Rasul, G.; Prakash, G. K. S. ¹H, ¹³C, ¹⁵N NMR and Theoretical Study of Protonated Carbamic Acids and Related Compounds. *J. Org. Chem.* **1998**, *63*, 7993–7998.
- (59) Gründler, F.; Scholz, H.; Herbig, M.; Schwarzer, S.; Wagler, J.; Kroke, E. Formation of Aromatic O-Silylcarbamates from Aminosilanes and Their Subsequent Thermal Decomposition with Formation of Isocyanates. *Eur. J. Inorg. Chem.* **2021**, 2021, 2211–2224.

☐ Recommended by ACS

Electronic Effect on Phenoxide Migration at a Nickel(II) Center Supported by a Tridentate Bis(phosphinophenyl)phosphido Ligand

Kunwoo Lee, Yunho Lee, et al.

FEBRUARY 08, 2023

INORGANIC CHEMISTRY

READ 🗹

Mechanistic Study of Alkyne Insertion into Cu-Al and Au-Al Bonds: A Paradigm Shift for Coinage Metal Chemistry

Diego Sorbelli, Paola Belanzoni, et al.

DECEMBER 09, 2022

INORGANIC CHEMISTRY

READ 🗹

Photoinduced Ligand-to-Metal Charge Transfer of Cobaltocene: Radical Release and Catalytic Cyclotrimerization

Keaton V. Prather and Emily Y. Tsui

JANUARY 26, 2023

INORGANIC CHEMISTRY

READ 🗹

PNCNP Pincer Platinum Chloride Complex as a Catalyst for the Hydrosilylation of Unsaturated Carbon-Heteroatom Bonds

Man Ding, Xuenian Chen, et al.

NOVEMBER 17, 2022

ORGANOMETALLICS

READ 🗹